

Accepted Manuscript

This is an Accepted Manuscript of the following article:

Branislav Vrana, Foppe Smedes, Ian Allan, Tatsiana Rusina, Krzysztof Okonski, Klára Hilscherová, Jiří Novák, Peter Tarábek, Jaroslav Slobodník. Mobile dynamic passive sampling of trace organic compounds: Evaluation of sampler performance in the Danube River. Science of The Total Environment. Volume 636, 2018, ISSN 0048-9697.

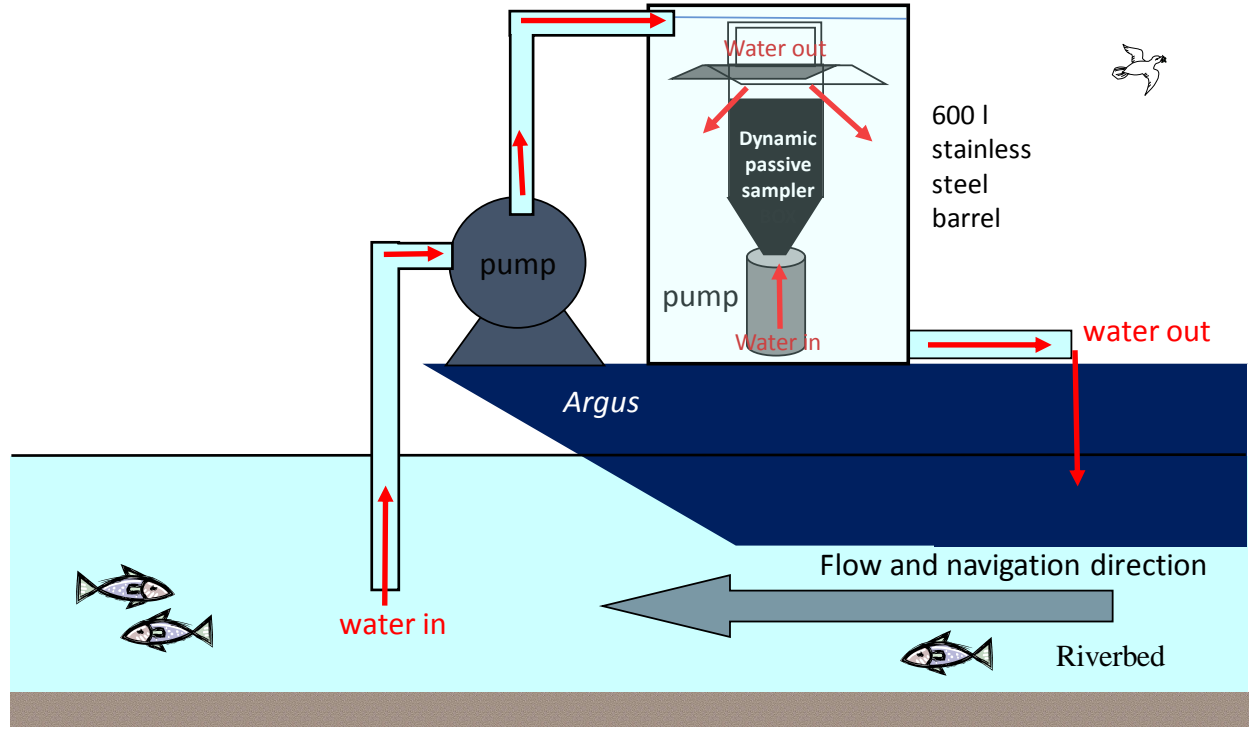
The article has been published in final form by Elsevier at
<http://dx.doi.org/10.1016/j.scitotenv.2018.03.242>

© 2018. This manuscript version is made available under the

CC-BY-NC-ND 4.0 license

<http://creativecommons.org/licenses/by-nc-nd/4.0/>

1 Graphical abstract



1 Mobile dynamic passive sampling of 2 trace organic compounds: evaluation of 3 sampler performance in the Danube 4 river

5 Branislav Vrana^{1*}, Foppe Smedes¹, Ian Allan², Tatsiana Rusina¹, Krzysztof Okonski¹, Klára Hilscherová¹,
6 Jiří Novák¹, Peter Tarábek³ and Jaroslav Slobodník⁴

7 ¹Masaryk University, Faculty of Science, Research Centre for Toxic Compounds in the Environment
8 (RECETOX), Kamenice 753/5, 625 00 Brno, Czech Republic

9 ²Norwegian Institute for Water Research, Gaustadalle´en 21, NO-0349 Oslo, Norway

10 ³Water Research Institute, Nábr. arm. gen. L. Svobodu 5, 81249 Bratislava, Slovakia

11 ⁴Environmental Institute, Okružná 784/42, 972 41 Koš, Slovakia

12 ***Corresponding author:**

13 Branislav Vrana

14 Research Centre for Toxic Compounds in the Environment (RECETOX)

15 Faculty of Science

16 Masaryk University

17 Kamenice 753/5, pavilon A29

18 625 00 Brno

19 Czech Republic

20

21 **tel:** +420 549 494 975

22 **e-mail:** vrana@recetox.muni.cz

23

24 **Keywords:** passive sampling, mass transfer, trace organic compounds, Joint Danube Survey, water
25 quality

26 **Highlights**

- 27
- A dynamic passive sampling device was designed to speed up the chemical uptake
 - The device was applied in the Danube river for sampling from a cruising ship
 - Spatially and temporally integrated samples of dissolved compounds were obtained
 - The device samples up to 5 times faster in comparison with a caged passive sampler
 - Mutual comparability of three passive samplers deployed in parallel was shown
- 30
- 31
- 32

33 **1 Abstract**

34

35 A “dynamic” passive sampling (DPS) device, consisting of an electrically driven large volume water
36 pumping device coupled to a passive sampler exposure cell, was designed to enhance the sampling
37 rate of trace organic compounds. The purpose of enhancing the sampling rate was to achieve
38 sufficient method sensitivity, when the period available for sampling is limited to a few days. Because
39 the uptake principle in the DPS remains the same as for conventionally-deployed passive samplers,
40 free dissolved concentrations can be derived from the compound uptake using available passive
41 sampler calibration parameters. This was confirmed by good agreement between aqueous
42 concentrations of polycyclic aromatic hydrocarbons (PAHs), polychlorinated biphenyls (PCBs) and
43 hexachlorobenzene (HCB) derived from DPS and conventional caged passive sampler. The DPS device
44 enhanced sampling rates of compounds that are accumulated in samplers under water boundary
45 layer control (WBL) more than five times compared with the conventionally deployed samplers. The
46 DPS device was deployed from a ship cruising downstream the Danube river to provide temporally
47 and spatially integrated concentrations. A DPS-deployed sampler with surface area of 400 cm² can
48 reach sampling rates up to 83 L d⁻¹. The comparison of three passive samplers made of different
49 sorbents and co-deployed in the DPS device, namely silicone rubber (SR), low density polyethylene
50 (LDPE) and SDB-RPS Empore™ disks showed a good correlation of surface specific uptake for
51 compounds that were sampled integratively during the entire exposure period. This provided a good
52 basis for a cross-calibration between the samplers. The good correlation of free dissolved PAHs, PCBs
53 and HCB concentration estimates obtained using SR and LDPE confirmed that both samplers are
54 suitable for the identification of concentration gradients and trends in the water column. We showed
55 that the differences in calculated aqueous concentrations between sampler types are mainly
56 associated with different applied uptake models.

57

58

59 2 Introduction

60 Organic compounds are often present in the water column of rivers and lakes at trace concentrations
61 that are difficult to detect when conventional low volume spot sampling of water is applied. Despite
62 the low concentrations, chemicals can present a significant risk to aquatic organisms and humans,
63 and many of them are regulated in surface waters (EU, 2013, 2000). Reliable and representative
64 monitoring is required for assessing compliance of water bodies with environmental quality
65 standards, or for characterizing spatial and temporal contamination trends.

66 Among available methods, passive sampling presents a promising approach to future regulatory
67 monitoring of trace organic compounds (Booij et al., 2016; Lohmann et al., 2012). Besides practical
68 advantages that include passive in situ concentration and preservation of sampled compounds in
69 sorbent materials, passive sampling provides freely dissolved compound concentrations, C_w (Vrana et
70 al., 2005). The C_w is considered to play a key role in understanding chemical's exposure of aquatic
71 organisms (Reichenberg and Mayer, 2006).

72 When conventional passive water samplers are applied, they must be deployed for several weeks or
73 months, because their ambient sampling rates (R_s), representing the volume of water extracted per
74 unit of time, are low. However, when the time period available for passive sampling is restricted,
75 compensation by high sampling rate is needed to sample a sufficient volume of water for
76 instrumental quantification or measuring chemical effects using bioanalytical tools.

77 Since R_s proportionally increase with the surface area of a sampler (Booij et al., 2007) they can be
78 increased by using samplers in the form of large thin sheets. Furthermore, R_s increase when the
79 water flow rate or turbulence on the sampler surface is higher (Estoppey et al., 2014; Li et al., 2010;
80 Vermeirssen et al., 2009; Vrana and Schüürmann, 2002). Faster flow conditions cause a thinner water
81 boundary layer (WBL) and lead to lower resistance to mass transfer (Levich, 1962). This is because the
82 mass transfer of hydrophobic compounds is typically controlled by their diffusion through the WBL
83 (Rusina et al., 2007). Flow turbulence can be increased by positioning samplers in a natural or
84 artificially created current, by shaking, rotating or vibrating them during exposure in water (Qin et al.,
85 2009). Allan et al. (2011) have shown increased R_s by towing samplers fastened to the end of a
86 benthic trawl net. In general, input of some external mechanical energy is needed for increasing the
87 water turbulence in vicinity of the samplers.

88 In this study, we investigated the applicability of a novel "dynamic" passive sampling device (DPS)
89 that was developed with the aim to maximize the sampling rates of pollutants by forcing water at
90 high flow rate along the passive sampler surface. The high flow was achieved by jetting water
91 through a narrow flow-through sampler exposure chamber using a pump. Hereto we 1) compared
92 the performance of DPS with conventional deployment of passive samplers in cages; 2) tested the
93 performance of the DPS device by deployment from a moving ship in the Danube river to obtain
94 integrated freely dissolved concentrations of pollutants in the water column over time and space; 3)
95 compared the uptake of compounds by silicone rubber, low density polyethylene and SDB-RPS
96 Empore™ disks samplers co-deployed inside the DPS device. The first two materials are commonly
97 used for sampling hydrophobic compounds, whereas the latter is used also for sampling hydrophilic
98 compounds. Finally, 4) we evaluated aqueous concentrations of atrazine derived from DPS in relation
99 to those from spot water sampling.

100

101

102

103 **List of terms and abbreviations**

104	A_x	sampler x surface area in contact with water
105	Caged passive sampler	a passive sampler deployed in a cage made of perforated stainless steel
106		sheet; It was deployed stationary in the Danube downstream Bratislava (see
107		Table 1).
108	DPS	Dynamic Passive Sampling device; a novel water sampling device which
109		forces water along the surface of sorbent sheets in a stainless steel flow-
110		through chamber. Water passes through the chamber at a high flow rate
111		assisted by a pump. This leads to a high turbulence close to the sorbent
112		surface, and therefore to higher sampling rates when compared to
113		conventional caged passive samplers.
114	D_x	diffusion coefficient of a compound in the phase x
115	DEQ_x	the degree of equilibrium that the compound attained during sampler x
116		exposure
117	δ_x	thickness of phase x
118	ED	Empore disk
119	$F_{ED/SR}$	the ratio of surface specific compound uptake in ED and SR samplers
120	GPC	gel permeation chromatography
121	HCB	hexachlorobenzene
122	$k_{o,x}$	overall mass transfer coefficient
123	k_w	mass transfer coefficient in the water boundary layer
124	k_x	mass transfer coefficient in the polymer x
125	K_{ow}	octanol-water partition coefficient
126	$K_{x,w}$	polymer x–water partition coefficient
127	LDPE	low density polyethylene
128	LOQ	limit of quantification
129	m_x	sampler mass
130	M	molar mass of a compound
131	Mobile deployment	deployment of a passive sampler from a moving object, e.g. from a ship
132	$N_{t,x}$	amount of a compound accumulated in the sampler x after exposure time t
133	OCPs	organochlorinated pesticides
134	PAHs	polycyclic aromatic hydrocarbons
135	PCBs	polychlorinated biphenyls
136	PRC	Performance Reference Compound(s).
137	RIS	recovery internal standard
138	$R_{s,x}$	sampling rate; the substance specific volume of water extracted per unit of
139		time
140	$^{300}R_{s,x}$	sampling rate for a compound with molar mass $M=300 \text{ g mol}^{-1}$
141	Spot water sample	samples of whole water that were collected using bottles from the
142		expedition ship at 63 sites in the 8 Danube stretches covered by passive
143		sampling. Spot samples reflect water quality only at the point in time that
144		the sample was collected.
145	Stationary deployment	deployment of a passive sampler at a fixed place.
146	SR	silicone rubber
147	WBL	water boundary layer

148 **3 Materials and Methods**

149 **3.1 Passive samplers**

150 Three types of passive samplers were applied: two partitioning samplers, SR and LDPE sheets and
151 one adsorption sampler based on styrene-divinylbenzene solid phase extraction disks, SDB-RPS
152 Empore™ disks (ED). AlteSil™ translucent SR sheets 0.5 mm thick (Altec, UK) were cut into samplers
153 with a size of 14×28 cm (392 cm², 23 g), Soxhlet extracted in ethylacetate for 72 h and spiked
154 according to the procedure described in Smedes and Booij (2012) with 14 performance reference
155 compounds (PRC: D₁₀-biphenyl and 13 polychlorinated biphenyl (PCB) congeners that do not occur in
156 technical mixtures; see Supplementary information (S1.2). LDPE (Brentwood Plastics Inc, St. Louis,
157 USA) strips of 4×28 cm (112 cm²) and 70 μm thickness were spiked with the 6 perdeuterated
158 polycyclic aromatic hydrocarbons (PAHs) as PRC (S1.2). An ED sampler consisted of ten 47 mm in
159 diameter Empore® SDB-RPS disks (Sigma Aldrich, Czech Republic), with a total mass of approximately
160 3.2 g and 173 cm² surface area. Before exposure, ED samplers were cleaned in acetone, isopropanol,
161 methanol and milliQ water, in which they were stored at 4 °C. ED samplers were not spiked with PRC.
162 Note that the stated total sampler surface area was nominal, while in practice 80% had contact with
163 water contact and ~20% was covered by the grid holding them in place.

164 **3.2 Water sampling**

165 **3.2.1 Sampling device**

166 The DPS device consists of a rectangular stainless-steel plate chamber with an open grid on both
167 sides. (Figures S1 and S2; Supplementary information). The different samplers were placed on the
168 grid (Figure 1) and covered by the lids. One end of the chamber was connected to a submersible
169 pump (approximately 9 m³ h⁻¹) that forced water at high flow velocity (1-2 m s⁻¹) through the
170 chamber while being immersed in the water. Temperature was monitored by a submersible logger
171 (Hobo Pendant, Onset, Germany) attached to the DPS device. The cruising speed of the ship did not
172 allow immersion of the DPS device directly in the river water and therefore it was immersed in a
173 flow-through system using a 600 L stainless steel tank positioned onboard the ship (Figure S3,
174 Supplementary information). The water was pumped through the tank at a rate of about 3 m³ h⁻¹
175 from a stainless-steel inlet tube positioned in front of the ship about 0.5 m below the water surface
176 (Figure S4, Supplementary information). Sampling by the DPS device on the ship did not decrease the
177 exposure concentration in the tank as its R_s of <100 L d⁻¹ was negligibly low in comparison with the
178 72000 L d⁻¹ flow through the tank.



179

Figure 1 Co-deployed AlteSil™ silicone rubber (SR sampler) and SDB-RPS Empore disks (ED sampler) and LDPE stripes (LDPE sampler) in a DPS device. The arrows show the direction of water streaming through the exposure chamber.

180

181 3.2.2 Deployment and retrieval

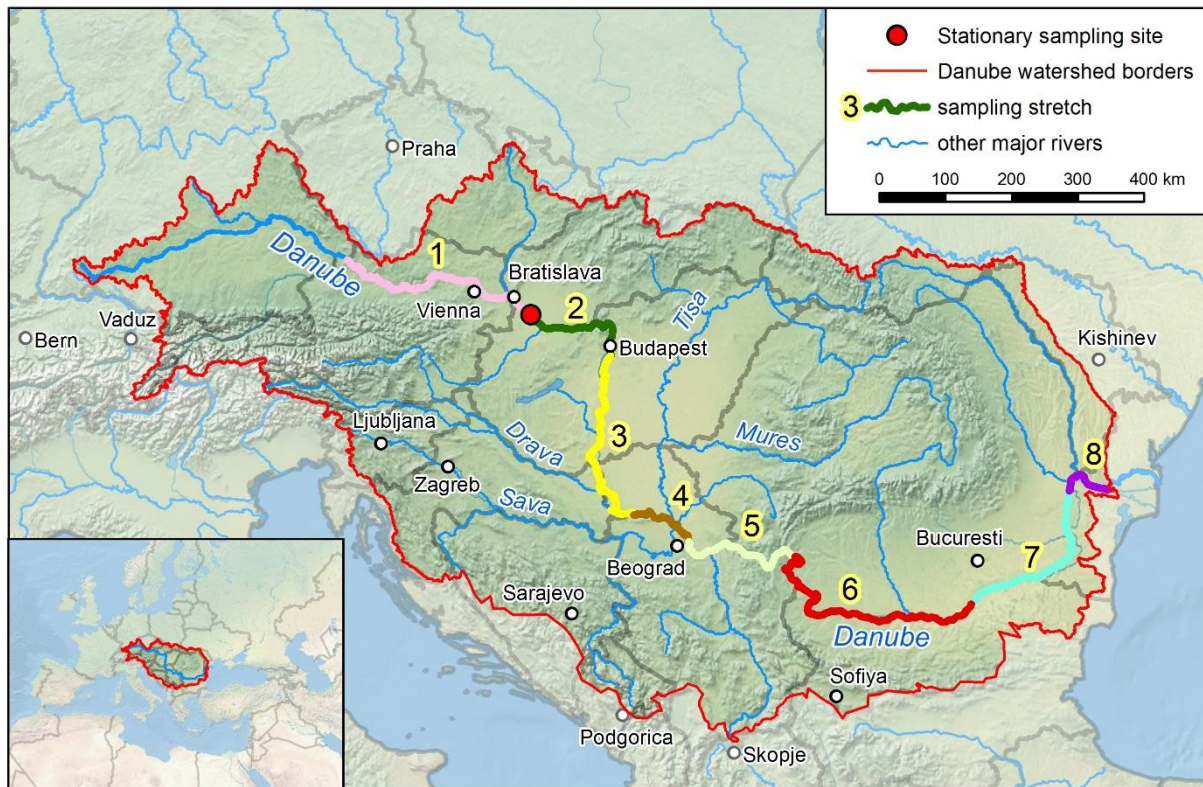
182 Samplers were always mounted in the DPS device just before exposure and retrieved immediately
 183 afterwards. Upon recovery, the surfaces of SR and LDPE samplers were cleaned using a pre-cleaned
 184 scourer and local river water. The surface of the ED samplers did not permit cleaning. Recovered
 185 samplers were placed back into their storage containers, stored at 4°C on board of the ship and
 186 transported to the laboratory within a week, and stored at -20°C until further processing. To estimate
 187 any contaminant uptake not associated with water exposure, field blank samplers were exposed to
 188 air in a stainless-steel tray during sampler's mounting and retrieval.

189 3.2.3 Sampling campaign

190 The sampling campaign was performed in August and September 2013 as part of the Joint Danube
 191 Survey 3 (JDS 3) by the expedition ship Argus (Liška et al., 2015). Passive sampling of organic
 192 compounds was performed over eight stretches of the Danube using the DPS device on board of the
 193 ship (Figure 2) in an approach similar to a FerryBox concept (Petersen, 2014) and the mobile
 194 continuous flow system (Petersen et al., 2016). Each individual water sampling period covered
 195 approximately 5 days, the time the ship moved downstream along a defined stretch. Note that the
 196 DPS was only in operation when cruising or anchored in the river. The device was always switched off
 197 before the ship entered harbours and switched on again when the cruise resumed. Consequently,
 198 actual sampling periods were about two days per stretch (Table 1).

199 During the period the ship sampled stretches 1 and 2, two subsequent stationary samplings of 4 and
 200 5 days each were conducted at a site located 1852 km distant from the Danube river mouth. They
 201 were performed from shore using a DPS device immersed in river water at the depth of
 202 approximately 1 m (Table 1 and Figure 2). In addition, a SR and an ED sampler were passively

203 deployed for 43 days (Table 1) in a perforated stainless steel cage (caged sampler). Unfortunately,
204 LDPE sampler deployed in cage was lost during sample transport.
205 Spot samples of surface water in bottles were also collected from the expedition ship at 63 sites in
206 the 8 Danube stretches covered by passive sampling. The time of spot sample collection within each
207 river stretch was always within the time period of passive sampler deployment (Table 1). A range of
208 priority substances was analysed in whole water samples by several expert laboratories (Deutsch and
209 Sengl, 2015). The results were reported to the International Commission for the Protection of the
210 Danube river and are accessible in a database (ICPDR International Commission for the Protection of
211 the Danube River, n.d.).



212 Figure 2 Map of the Danube river stretches and the stationary station (the red circle) passively
sampled in August and September 2013. Details of sampling in individual stretches are given in Table
1.

213

Table 1 Meta data for sampling from the Argus ship at the various Danube river stretches and a stationary station in August and September 2013.

Stretch	Stretch start and end	River km ¹	Dates of cruise and sampler deployment	Mean water temperature [°C]	Exposure time [d]
S1	Passau-Bratislava	2203-1852	17.8.-22.8.	21.3	2.0
<i>Stationary deployment; DPSa²</i>	<i>Downstream Bratislava</i>	<i>1852</i>	<i>19.8.-23.8.</i>	<i>21.3</i>	<i>4.0</i>
<i>Stationary deployment; DPSb²</i>	<i>Downstream Bratislava</i>	<i>1852</i>	<i>23.8.-28.8.</i>	<i>21.3</i>	<i>5.0</i>
<i>Stationary deployment; Caged sampler</i>	<i>Downstream Bratislava</i>	<i>1852</i>	<i>28.8.-10.10.</i>	<i>20.0</i>	<i>43</i>
S2	Bratislava-Budapest	1852-1632	22.8.-26.8.	22.0	1.2
S3	Budapest-Vukovar	1648-1297	26.8.-2.9.	21.9	1.7
S4	Vukovar-Belgrade	1297-1154	2.9.-6.9.	22.8	1.6
S5	Belgrade-Turnu-Severin	1154-930	6.9.-10.9.	22.1	2.0
S6	Turnu-Severin-Ruse	930-495	11.9.-17.9.	21.9	2.0
S7	Ruse-Braila	495-170	17.9.-21.9.	19.2	1.4
S8	Braila-Tulcea	170-71	21.9.-26.9.	18.7	1.3

214 ¹The distance from the river mouth. ²the two subsequent stationary deployments of a DPS are labeled as DPSa and DPSb, respectively.

215 3.3 Sampler analysis

216 3.3.1 Silicone rubber (SR) sheets

217 Exposed, field blank, and control SR samplers, were spiked with SR recovery internal standards (SR
 218 RIS; section 2.2. in Supplementary information) and Soxhlet extracted for 8 hours with methanol. The
 219 extract was concentrated by Kuderna-Danish (KD) apparatus to 4 mL, dried over anhydrous Na₂SO₄,
 220 and further concentrated to 2 mL under a gentle nitrogen flow. A 20 % aliquot was used for analysis
 221 of alkyl phenols and polar compounds by LC/MS methods. Twenty mL hexane was added to the
 222 remaining extract, and methanol was azeotropically removed by KD concentration. An aliquot
 223 representing 20% of the total extract in hexane was further cleaned-up over a silica gel column by
 224 elution with diethyl ether/acetone, and used for analysis of PAHs and other target groups of
 225 compounds. The remaining 60% was purified using activated silica gel modified with sulphuric acid
 226 for the analysis of OCPs, PCBs, PRCs and other halogenated compounds. After addition of syringe
 227 internal standards (IS) and volume reduction both extracts were analysed by GC-MS/MS (section 2.3
 228 in Supplementary information).

229 3.3.2 Low density polyethylene (LDPE) sheets

230 All LDPE samplers, including field controls, were extracted twice by soaking overnight with *n*-pentane
 231 (100 mL) after addition of LDPE RIS (section 2.2 in Supplementary information). The volume of
 232 pentane was reduced to 2 mL by a gentle stream of nitrogen at room temperature. Extracts were
 233 first split into two equal fractions by volume. One fraction received a general clean-up using gel
 234 permeation chromatography (GPC). This post GPC sample was again split into two equal fractions by
 235 volume; the first of these fractions was reduced in volume using nitrogen and analysed for PAHs; the
 236 second one received treatment with 2×1 mL concentrated sulphuric acid, was reduced in volume,
 237 and analysed for PCBs and OCPs. Details of the procedure and instrumental analysis are described in
 238 (Allan et al., 2013).

239
 240

241 3.3.3 Empore disks

242 All ED samplers for chemical analysis were spiked with ED RIS (Supplementary information). Samplers
243 were then freeze dried for 24 hours in the original storage and transport containers and extracted
244 three times by slow shaking (12 h) at room temperature with 70 ml acetone. The volume of
245 combined extracts was reduced by vacuum rotary evaporation and, after removal of particles by
246 filtration through a layer of anhydrous Na₂SO₄, further reduced in volume to approximately 1 mL.
247 Solvent transfer to methanol was performed by addition of methanol (20 ml) and subsequent volume
248 reduction to 2 mL by a nitrogen flow. Aliquots were used for various instrumental analytical
249 methods. An aliquot representing 10% of the total extract was further azeotropically solvent
250 exchanged by KD to hexane for analysis of PAHs.

251 3.4 Data analysis

252 3.4.1 Sampling rate – theory

253 The compound sampling rate of a sampler made of polymer x, $R_{s,x}$, represents the volume of water
254 extracted per unit of time. Compound diffuses to the sampler through the WBL and the polymer
255 membrane comprising the sampler (Booij et al., 2007), and is finally sorbed. The overall resistance to
256 mass transfer, i.e. the reciprocal value of the overall mass transfer coefficient, $k_{o,x}$, can be expressed
257 as the sum of the transport resistances in WBL and polymer:

$$\frac{1}{k_{o,x}} = \frac{1}{k_w} + \frac{1}{k_x K_{x,w}} \quad \text{Equation 1}$$

258 where k_w and k_x are the mass transfer coefficients in the WBL and the membrane (made of
259 polymer x), respectively, and $K_{x,w}$ is the polymer x–water partition coefficient. The transport
260 resistances for a compound through WBL and membrane, are inversely proportional to the diffusion
261 coefficients, D_w and D_x , and proportional to their thicknesses δ_w and δ_x , respectively. Compounds,
262 however, do not only simply diffuse through the membrane but are also accumulated in the
263 membrane. The diffusion pathlength in the membrane can be approximated using $0.5 \times \delta_x$ (Salaun and
264 Buffle, 2004; Ter Laak et al., 2008). Consequently, Equation 1 transforms to:

$$\frac{1}{k_{o,x}} = \frac{\delta_w}{D_w} + \frac{0.5 \delta_x}{K_{x,w} D_x} \quad \text{Equation 2}$$

265 Finally, the product of the mass transfer coefficient and sampler- surface area in contact with water
266 (A_x) equals the sampling rates $R_{s,x}$ (L d⁻¹) as

$$R_{s,x} = k_{o,x} A_x = \frac{A_x}{\frac{1}{k_w} + \frac{0.5 \delta_x}{K_{x,w} D_x}} \quad \text{Equation 3}$$

267 Membrane-controlled mass transfer has to be considered especially for compounds with low $K_{x,w}$,
268 since the transport resistance is inversely proportional to the $K_{x,w}$, and, as a result, for less
269 hydrophobic compounds the transport resistance in polymer often controls the uptake rate (Booij et
270 al., 2007). In case the transport resistance in polymer is negligible, equation 3 reduces to

$$R_{s,x} = k_w A_x = \frac{D_w}{\delta_w} A_x \quad \text{Equation 4}$$

271 The latter term follows from equation 2 showing R_s 's dependence on the turbulence represented by
272 δ_w and compound's specific D_w . These two factors were captured in a model (Rusina et al., 2010):

$$R_{s,x} = A_x k_w = A_x BM^{-0.47} \quad \text{Equation 5}$$

273 where M is the molar mass (g mol^{-1}) inserting effect of D_w and B an exposure specific proportionality
274 factor representing the flow conditions and containing the factor for unit conversion. Sampling rate
275 calculation

276 For SR and LDPE samplers, in-situ sampling rates were estimated using retained PRC fractions $f(\text{PRC})$
277 as the ratio between PRC concentrations in the sampler after exposure time t and at $t = 0$. The
278 modelled retained fraction is a function of exposure time t and $K_{x,w}$. following:

$$f(\text{PRC}) = \exp\left(-\frac{R_{s,x}t}{K_{x,w}m_x}\right) \quad \text{Equation 6}$$

279 Where m_x is the sampler mass. After inserting equation 5 into equation 6, modeled $f(\text{PRC})$ are fitted
280 to measured $f(\text{PRC})$ using nonlinear regression with B as adjustable parameter (Booij and Smedes
281 2010). Compound specific $R_{s,x}$ were then calculated using equation 5 as shown for SR in Figure S5 in
282 Supplementary information.

283 When also membrane-controlled mass transfer has to be considered equation 3 can be inserted in
284 equation 6 and $R_{s,x}$ calculated applying a similar fitting with k_w as adjustable parameter.
285 Because the ED sampler is an adsorption-based sampler, desorption kinetics are generally not
286 isokinetic with the uptake. Therefore, calculation of sampling rates for the ED sampler from PRC
287 elimination cannot be applied (Shaw et al., 2009). For compounds under investigation with assumed
288 integrative uptake the $R_{s,ED}$ of ED samplers were derived from a correlation of uptake of PAHs and
289 nonylphenol by ED and SR samplers as shown in the Results section.

290 **3.4.2 Models for calculating sampling rates in LDPE sheets**

291 Three approaches were tested to estimate sampling rates for LDPE sheets.

292 'A', we assumed equality of WBL-controlled mass transfer coefficients in SR and LDPE samplers, and
293 therefore mass transfer coefficients derived for SR samplers were applied to the LDPE samplers.
294 $R_{S,LDPE}$ values were then calculated using equation 3 using the $k_w = BM^{0.47}$ derived from PRC dissipation
295 from SR (equation 5). The required D_{LDPE} and $K_{LDPE,w}$ values were taken from (Rusina et al., 2010) and
296 (Smedes et al., 2009).

297 'B', $R_{S,LDPE}$ was calculated from PRC dissipation using the combination of equations 3 and 6 and
298 resistances to mass transfer in both WBL and polymer were modelled as a function of compound
299 hydrophobicity using the model proposed by (Booij et al., 2003). Details of the model are given in
300 paragraph 2.5 in Supplementary information.

301 'C', WBL controlled R_s was calculated from dissipation data of d_{12} -CHR and d_{12} -BeP using the
302 combination of equations 5 and 6. Only two PRCs could be included in the model, since the
303 remaining PRCs either completely dissipated from the sampler or their release was partially
304 controlled by the membrane. $R_{S,LDPE}$ values were then calculated using equation 3.

305 **3.4.3 Estimation of free dissolved concentration in water**

306 Uptake of analytes absorbed by the samplers follows a first-order approach to equilibrium. DEQ_x is
307 the degree of equilibrium that the chemical attained during sampler exposure:

$$DEQ_x = \left(1 - \exp\left(-\frac{R_{s,x}t}{K_{x,w}m_x}\right) \right) \quad \text{Equation 7}$$

308 The uptake can be considered integrative until DEQ_x reaches the value of 0.5. The required $K_{x,w}$ values
 309 of PAHs and PCBs in SR/water and LDPE/water system are available from (Smedes et al., 2009).
 310 Aqueous concentrations $C_{w,x}$ for SR and LDPE samplers were calculated from the mass absorbed by
 311 the samplers N_x , the in situ sampling rate ($R_{s,x}$) of the chemicals and their sampler-water partition
 312 coefficients $K_{x,w}$ as described in (Booij et al., 2007):

$$C_{w,x} = \frac{N_x}{K_{x,w} m_x DEQ_x} \quad \text{Equation 8}$$

313 Aqueous concentrations $C_{w,ED}$ for ED samplers were calculated according to (Booij et al., 2007),
 314 assuming a linear uptake mode during the entire exposure:

$$C_{w,ED} = \frac{N_x}{R_{s,ED}t} \quad \text{Equation 9}$$

315 However, for prolonged exposure times the extracted volume is constrained by the uptake capacity
 316 of the passive sampler ($K_{ED,w} \times m_{ED}$) and in such case, Equation 8 should be applied, that considers
 317 equilibration of sampler with the sampled water. Unfortunately, published $K_{x,w}$ values for ED are rare
 318 and currently not available for PAHs and alkylphenols.

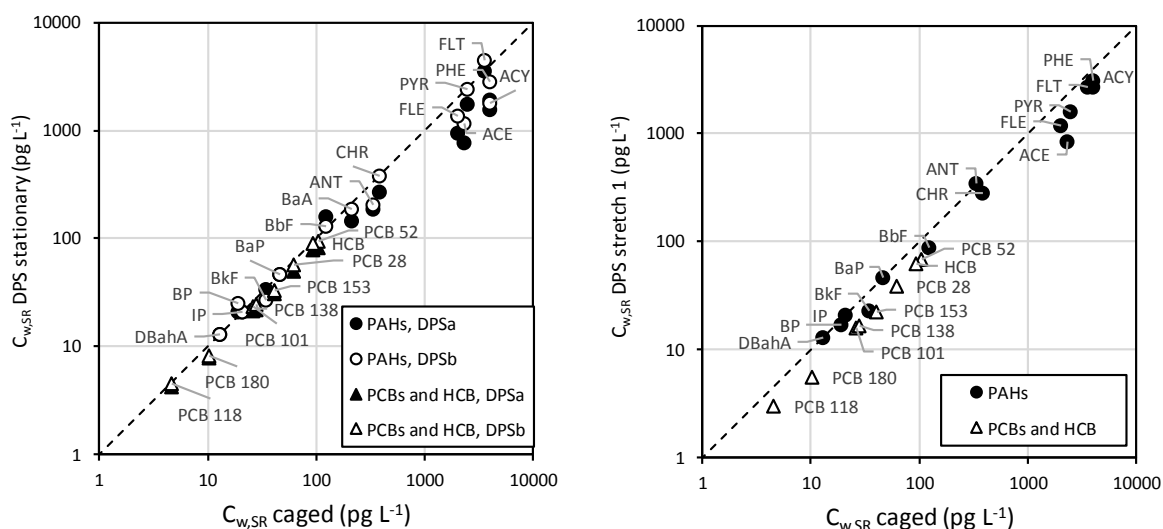
319 **4 Results and discussion**

320 **4.1 Performance of the DPS device**

321 **4.1.1 Comparison of caged sampler and DPS**

322 The $C_{w,SR}$ of PAHs, PCBs and HCB were calculated using analyte amounts accumulated in SR and the
 323 $R_{s,SR}$ obtained as described in section 3.4. The $C_{w,SR}$ for stationary caged samplers and stationary DPS
 324 devices downstream Bratislava agreed very well (Figure 3, left graph), with a median ratio of 0.93
 325 and 0.83 for individual PAHs and PCBs, respectively. Similarly, a reasonably good median $C_{w,SR}$ ratio
 326 was obtained for individual PAHs and PCBs from caged samplers and mobile passive samplers in the
 327 stretch between Passau-Bratislava (Figure 3, right graph), namely 0.74 and 0.61, respectively. In both
 328 cases the largest differences were observed for PAHs with two and three aromatic rings, which were
 329 present in water at highest concentrations.

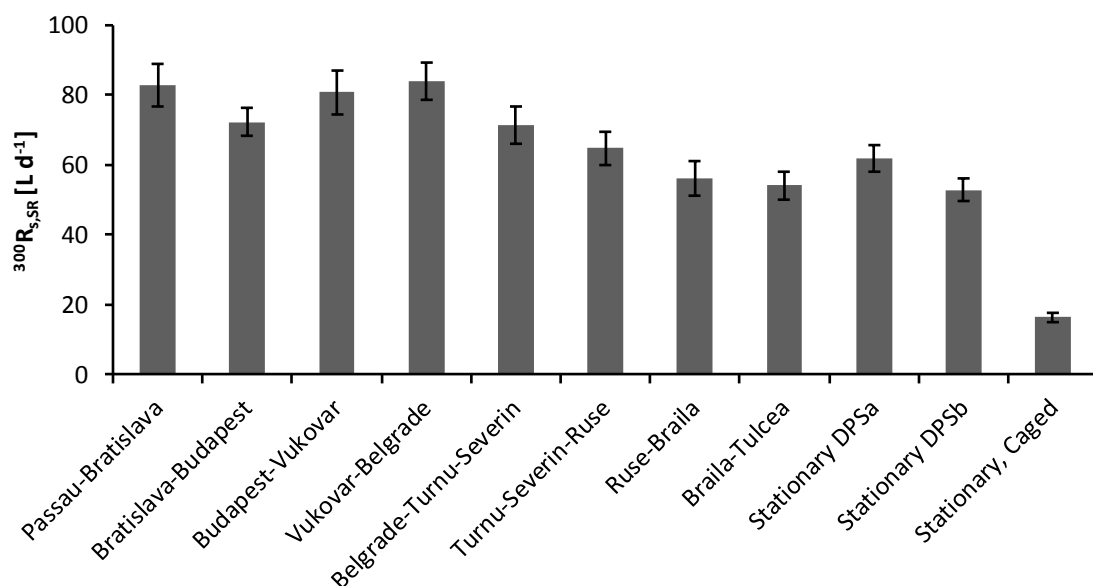
330 The good $C_{w,SR}$ agreement was observed despite different sampling rates and water volumes sampled
 331 by the caged and DPS device mounted samplers. From our previous experience with passive sampling
 332 (Vrana et al., 2014) and based on reported PCB concentrations bound to suspended particulate
 333 matter (Umlauf et al., 2015), concentrations of PAHs and PCBs in the Danube water were not
 334 expected to fluctuate dramatically. Assuming low temporal variation of $C_{w,SR}$, observed differences in
 335 uptake are mainly related to the chemical's DEQ_{SR} (equation 7) attained in different samplers. For
 336 selected PAHs, PCBs and HCB, Figure S6 in Supplementary information shows that when uptake
 337 during the different samplings are inter-connected by a line, the curves resemble linear relation with
 338 DEQ_{SR} up to 0.5 and an exponential rise to a maximum as DEQ_{SR} approaches 1.



339
 340 Figure 3. Comparison of concentrations in water $C_{w,SR}$ (pg L⁻¹) of selected PAHs (circles), PCBs and HCB
 341 (triangles) derived from uptake in caged SR passive samplers at a stationary site (x-axis data) with
 342 data from stationary DPS (left graph) and mobile DPS(right graph). The dashed lines represent
 343 equality of the plotted variables. Details of exposures are given in Table 1. Compound abbreviations
 344 are explained in Supplementary information, Table S1.
 345

346 4.1.2 Evaluation of DPS sampling rates during the Danube cruise

347 The $^{300}R_{s,SR}$ (R_s for a compound with molar mass $M=300$ g mol⁻¹) took the value of 83, 62 and 53 L d⁻¹
 348 for the mobile DPS along stretch 1, and the two stationary DPS exposures, respectively (Figure 4).
 349 Meanwhile, $^{300}R_{s,SR}$ was only 16 L d⁻¹ for the caged sampler, although it had the same area A_x and was
 350 deployed in a rapid river current with a flow velocity of approximately 1 m s⁻¹. Even much lower
 351 sampling rates are envisaged with caged samplers in stagnant waters. Thus, the DPS device can
 352 increase R_s by more than 5-fold in comparison with the caged samplers. This is extremely useful
 353 when ultra trace compounds need to be enriched within a short time.
 354 During the ship cruise $^{300}R_{s,R}$ decreased by up to 35%, from 83 to 54 L d⁻¹ (Table S2; Figure 4). Using
 355 the available data on temperature dependence of SPMD sampling rates (Vrana et al., 2014), the
 356 decrease of temperature from 23 to 19°C is expected to result in a reduction of aqueous diffusion
 357 leading to lower mass transfer through the WBL by approximately 20%. Indeed, $^{300}R_{s,SR}$ is correlated
 358 with water temperature during the cruise ($R=0.81$). The remaining 15% decrease in $^{300}R_{s,SR}$ may be
 359 related to the decreasing effectiveness of the pump on DPS device during continuous operation over
 360 2 months. The lower DPS sampling rates at the stationary site can be explained by a possible negative
 361 effect of river current, reducing the suction pressure of the submersible pump in the DPS device. In
 362 contrast, the mobile DPS device was positioned in a barrel with a constant hydrostatic pressure and
 363 no other water flow than that created by the pump itself.



364

Figure 4 Comparison of sampling rates ($^{300}R_{s,SR}$ value of a model compound with a molar mass of 300 g mol⁻¹) of SR samplers deployed in the DPS device at various stretches and, one stationary station with two DPS deployments and one caged deployment.

365

Table 2. Uptake parameters for compounds detected above their limit of quantification in SR and LDPE samplers. $R_{s(m)}$ is a hypothetical sampling rate in a situation when the compound uptake is fully controlled by diffusion in polymer membrane. $R_{s,x}$ shows the range of in situ sampling rates determined during exposure of samplers in the Danube river. $R_{s,LDPE}$ were calculated using method 'A' outlined in 3.4.2.

Compound	Abb.	Log K_{ow}	Samp-ler	¹ log $K_{x,w}$ (L kg ⁻¹)	² log D_x (m ² s ⁻¹)	δ_x (μm)	A (cm ²)	$R_{s(m)}$ (L d ⁻¹)	$R_{s,x}$ (L d ⁻¹)	$k_{o,x}$ (μm s ⁻¹)
Phenan-threne	PHE	4.57	SR	4.11	-10.18	500	392	11530	68-108	20-32
			LDPE	4.22	-12.45	70	112	163	17-25	18-26
Fluoran-thene	FLT	5.22	SR	4.62	-10.40	500	392	22483	64-101	19-30
			LDPE	4.93	-12.75	70	112	470	17-27	18-27
Pyrene	PYR	5.18	SR	4.68	-10.40	500	392	25814	64-101	19-30
			LDPE	5.10	-12.82	70	112	527	17-27	18-27
Chrysene	CHR	5.86	SR	5.25	-10.61	500	392	59137	60-94	18-28
			LDPE	5.78	-13.28	70	112	874	17-26	17-27
PCB 28	PCB 28	5.67	SR	5.53	-10.13	500	392	340298	57-90	17-27
			LDPE	5.40	-12.51	70	112	2146	16-25	17-26
Hexachloro-benzene	HCB	5.50	SR	5.05	-10.12	500	392	115308	54-86	16-25
			LDPE	5.43	-12.68	70	112	1555	15-24	16-25

366 ¹ Values of $K_{SR,w}$ and $K_{LDPE,w}$ were taken from (Smedes et al., 2009); ² Values of log D_x were taken from
 367 Rusina et al. (2010)

368

369 To verify that the uptake was WBL controlled for the entire hydrophobicity range under deployment
370 conditions in SR and LDPE samplers, the overall sampling rate $R_{s,x}$ should be much lower than the
371 estimated sampling rate $R_{s(m)}$ if controlled by diffusion in polymer:

$$R_{s,x} \ll R_{s(m)} \approx \frac{D_x K_{x,w} \rho_x A_x}{0.5 \delta_x} \quad \text{Equation 10}$$

372 where ρ_x is the density of polymer. The calculation confirmed that in both samplers and in all
373 exposures, mass transfer was dominantly WBL controlled for all compounds (Table 2).

374 **4.2 Comparing uptake by three co-deployed passive samplers**

375 Mutual comparison of compound uptake in the three co-deployed samplers is useful to reveal
376 similarities or differences in mass transfer mechanisms and partition equilibria of compounds in
377 different samplers. The sampler inter-comparability is based on a rationale of the same underlying
378 principles for the compound mass transfer from water to SR, LDPE and ED passive samplers.
379 Moreover, in the DPS devices all three sampler types were one sided exposed in the same
380 arrangement as flat sheets or disks that were flushed with river water at a constant flow velocity
381 (Figure 1). However, the samplers differed in surface area, thickness and shape of sheets/disks, the
382 quality and mass of polymer or sorbent material applied.

383
384 Since in the integrative uptake phase the amount of a compound accumulated in the sampler $N_{t,x}$ is
385 proportional to the sampling rate ($N_{t,x} = C_{w,x} \times R_{s,x} \times t$) and that in turn is proportional to sampler surface
386 area A_x (Kees Booij et al., 2007), consequently, the surface specific compound uptakes $N_{t,x}/A_x$
387 (ng cm^{-2}) are expected to be mutually comparable.

388 **4.2.1 Comparison of surface specific uptake in SR and LDPE**

389 Among the measured compounds, quantifiable concentrations were found in all exposed SR and
390 LDPE samplers only for six compounds: phenanthrene (PHE), fluoranthene (FLT), pyrene (PYR) and
391 chrysene (CHR), hexachlorobenzene (HCB) and PCB 28. The remaining PCBs and PAHs were
392 quantifiable in SR, but mostly below the LOQ in LDPE samplers. The lower uptake to LDPE in
393 comparison to SR is related to its 3.5-times lower surface area and its 30-times lower mass, which
394 results in lower sampling rates and lower uptake capacity ($K_{x,w} \times m_x$), respectively (Booij et al., 2017).
395 The $N_{t,x}/A_x$ in LDPE and SR passive samplers and their ratios are shown in Figures S7 and S8 in
396 Supplementary information, respectively. Except for CHR, the $N_{t,SR}/A_{SR}$ was higher than $N_{t,LDPE}/A_{LDPE}$.
397 The highest deviations of the ratio from unity were observed for PHE (5.1 to 14.2), FLT (1.5 to 4.6),
398 and PYR (1.1 to 2.6). For CHR the ratio ranged from 0.5 to 1.1. Ratio values 1.1 to 1.8 and 1.2 to 2.4
399 were observed for HCB and PCB 28, respectively. The observed differences in $N_{t,x}/A_x$ can be caused
400 either by a different degree of partitioning equilibrium reached in LDPE and SR samplers (Figure S9 in
401 Supplementary information) or by a difference in the mass transfer controlling resistance (WBL vs.
402 membrane controlled uptake).

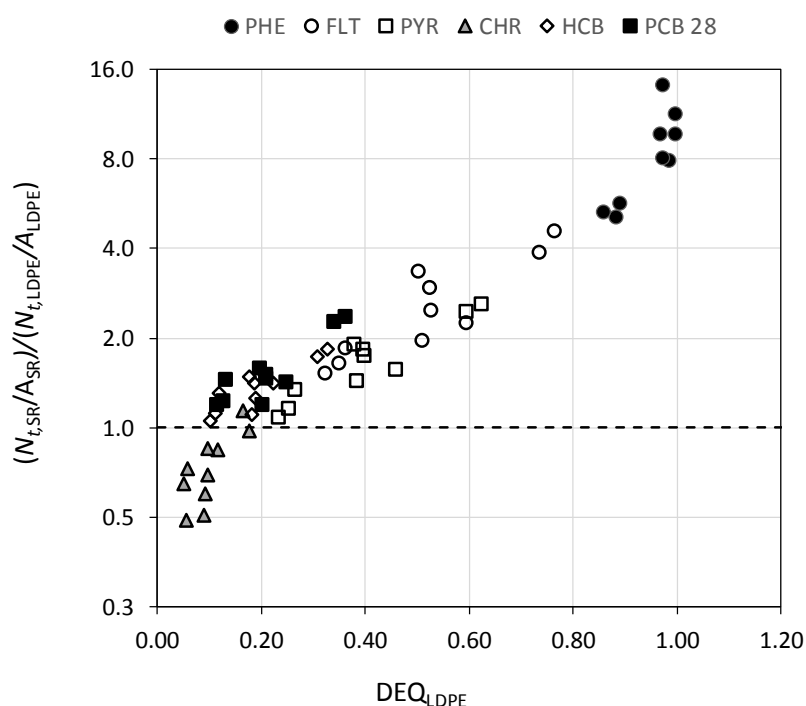
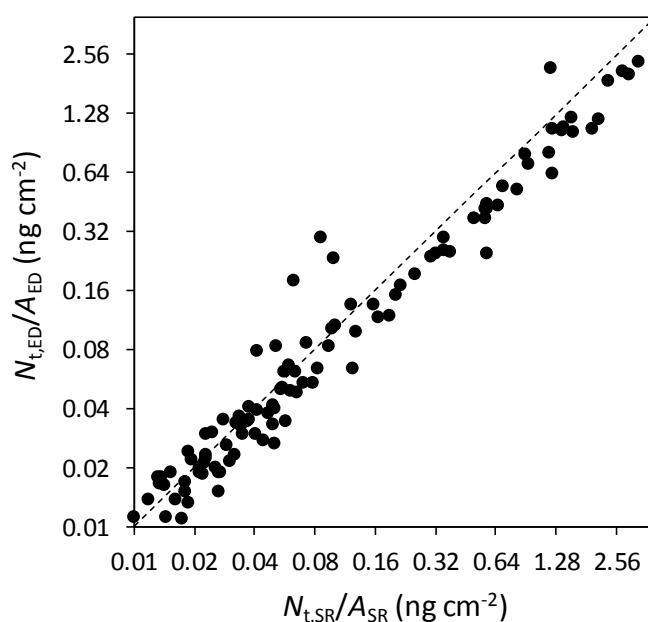


Figure 5. Ratio of surface specific uptake of selected PAHs, PCB 28 and HCB in SR and LDPE samplers as related to the degree of equilibrium with water reached by the LDPE sampler (DEQ_{LDPE}). The dashed line represents the ratio equal to unity. DEQ_{LDPE} was calculated using method 'A' outlined in 3.4.2.

403 Since integrative uptake to SR was observed for all compounds (i.e. $DEQ_{SR} < 0.5$ in most cases), the
 404 ratio of $N_{t,x}/A_x$ in SR and LDPE was drawn against the DEQ_{LDPE} , where curvilinear uptake phase of
 405 compounds was reached in many exposures (Figure 5). The graph shows that for all compounds the
 406 $N_{t,x}/A_x$ ratio increases with the increasing DEQ_{LDPE} , but remains close to unity (within approximately a
 407 factor of two) where the sampling is integrative in both samplers, i.e. when $DEQ_{LDPE} < 0.5$. Higher
 408 $N_{t,x}/A_x$ in SR than in LDPE of PHE and FLT uptake is related to a longer integrative sampling in SR
 409 compared to LDPE.

410 4.2.2 Comparison of surface specific uptake in SR and ED

411 The surface specific uptake ($N_{t,x}/A_x$) in ED and SR was compared for PAHs and nonylphenol, since they
 412 were well measurable in both samplers. In SR, integrative uptake was observed for compounds with
 413 $\log K_{SR,w} > 4.5$ during the entire exposure period in all exposed samplers; i.e. for 10 PAHs with more
 414 than three aromatic rings in their molecule, as well as for 4-nonylphenol (Figure S10 in
 415 Supplementary information). The comparison was performed for these compounds. The $N_{t,x}/A_x$ in SR
 416 and ED samplers showed a very good correlation for the selected substances (Figure 6). The
 417 comparison of surface specific uptake in individual sampler exposures is shown in detail in
 418 Supplementary information (Figure S11).



419

Figure 6. Surface specific uptake of PAHs with $\log K_{SR,w} > 4.5$ and 4-nonylphenol (11 substances) in ED versus SR passive samplers deployed in DPS devices in 8 mobile and 2 stationary deployments. The dashed line indicates unity.

420 A ratio $F_{ED/SR}$ of surface specific compound uptake in both samplers was calculated as:

$$F_{ED/SR} = \frac{N_{t,ED}/A_{ED}}{N_{t,SR}/A_{SR}} \quad \text{Equation 11}$$

421 The $F_{ED/SR}$ for the selected substances was close to unity and the overall median value was 0.83. The
 422 median value of $F_{ED/SR}$ for individual substances ranged from 0.7 to 1.2 for benzo[e]pyrene and
 423 benz[a]anthracene, respectively (Figure S12, Supplementary information). The highest $F_{ED/SR}$
 424 variability was mainly observed for compounds with the concentrations in passive samplers close to
 425 limit of quantification. The $F_{ED/SR}$ did not show any significant trend with the concentration level
 426 in samplers or with $K_{SR,w}$ values of test compounds (Figure S13, Supplementary information). Thus, we
 427 assume that the observed variability of $F_{ED/SR}$ for different compounds and different exposures is
 428 caused mainly by analytical variability. In conclusion, the good correlation of $N_{t,x}/A_x$ in various
 429 compared samplers for compounds that are sampled integratively provides an excellent basis for a
 430 robust cross-calibration between the samplers.

431 4.2.3 Comparison of C_w derived from uptake to SR and LDPE

432

433 In the next step we evaluated the agreement of $C_{w,x}$ values derived from compound uptake in SR and
 434 LDPE samplers. Since comparable surface specific uptake ($N_{t,x}/A_x$) in the two samplers was observed
 435 for chemicals under WBL control, the differences in calculated $C_{w,x}$ values for those chemicals should
 436 be mainly attributed to the differences in the models applied for $C_{w,x}$ calculation.

437 $C_{w,SR}$ were calculated using the approach outlined in 3.4.1 and 3.4.3 and three different models

438 (3.4.2) were applied for interpretation of uptake data from LDPE sampler. $C_{w,LDPE}$ data obtained using

439 the three models were then checked for consistency with $C_{w,SR}$ data (Figure S14, Supplementary
440 information). For all compounds with exception of PHE and FLT, a very good correlation (correlation
441 coefficient R between 0.74 and 0.96) was found between $C_{w,x}$ values derived from the two samplers.
442 The lower correlation for PHE ($R=0.62$) and FLT ($R=0.57$) was most likely caused by the shorter
443 integrative uptake in LDPE in comparison with SR. . Although the two samplers were co-deployed for
444 the same time period, the calculated $C_{w,LDPE}$ and $C_{w,SR}$ represent time-weighted average values over
445 differing time periods. The good correlation of $C_{w,x}$ estimates obtained using the two passive
446 samplers indicates that both samplers are suitable for the identification of concentration gradients
447 and the assessment of compound trends in water column, e.g. along the Danube river.
448 However, the application of different models for calculation of $C_{w,LDPE}$ introduced various levels of
449 systematic difference from the $C_{w,SR}$ estimates. Among the approaches tested, 'A' provided the best
450 consistency of the results between the compared SR and LDPE samplers (Figure 7) with the median
451 $C_{w,SR}/C_{w,LDPE}$ ratio ranging from 0.7 for CHR to 2.2 for PHE. In contrast, the 'B' and 'C' options resulted
452 in $C_{w,LDPE}$ values that were systematically lower than $C_{w,SR}$. In the case of model 'B', the median
453 $C_{w,SR}/C_{w,LDPE}$ ratio ranged from 1.4 for CHR to 3.5 for PCB 28. In the case of approach 'C', the median
454 $C_{w,SR}/C_{w,LDPE}$ ratio ranged from 2.2 for CHR to 4.4 for PCB 28.

455
456 To investigate the origin of differences in $C_{w,x}$ estimates, overall mass transfer coefficients $k_{o,x}$ of
457 compounds accumulated in samplers were calculated as surface specific sampling rates ($k_{o,x}=R_{s,x}/A_x$).
458 The required sampling rates were calculated from PRC release data using various models outlined in
459 3.4. The comparison of calculated $k_{o,x}$ values is shown in Figure S15 in Supplementary information
460 and in Table 2 (for results from model 'A' in 3.4.2, only). When models 'B' and 'C' were applied for
461 calculation of $k_{o,LDPE}$, the calculated $k_{o,LDPE}/k_{o,SR}$ ratio is systematically higher than one (1.2 to 5.1) and
462 in both models its value increases with increasing compound hydrophobicity or molar mass. Results
463 of these two model calculations contradict the observed generally higher surface specific uptake in
464 SR in comparison with LDPE (Figure S8). The model 'A' calculates $k_{o,LDPE}$ for WBL controlled uptake to
465 be equal to $k_{o,SR}$, and thus the $k_{o,LDPE}/k_{o,SR}$ ratio for all compounds excepting PHE is very close to unity
466 (Figure S15).

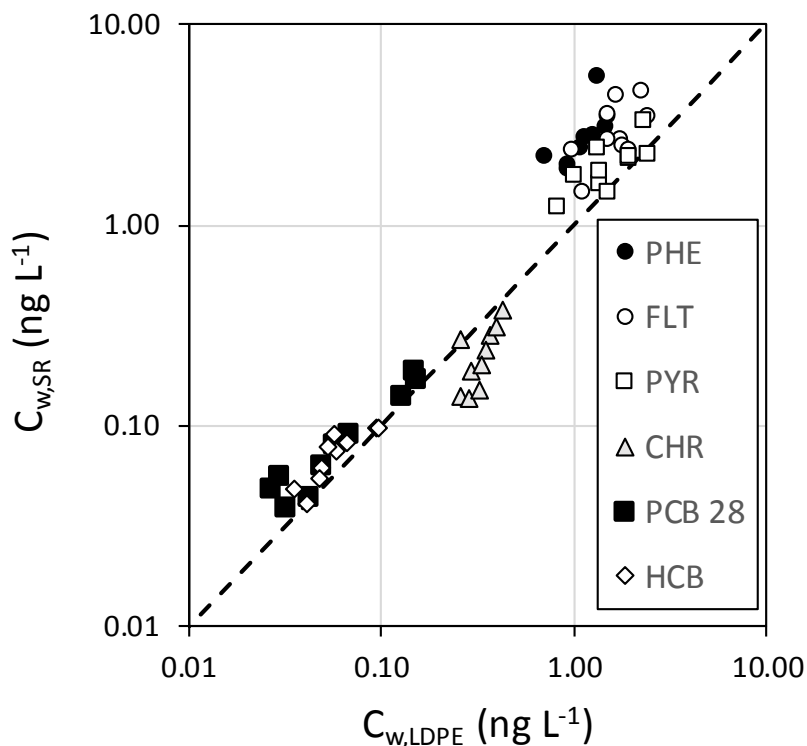
467
468 There are several factors that contribute to the systematic discrepancy between $k_{o,LDPE}$ values under
469 WBL control obtained using models 'B' and 'C', and $k_{o,SR}$ values used in the model 'A'.

470 The model 'B' calculates $k_{o,LDPE}$, including resistances in WBL and membrane as a function of
471 hydrophobicity, represented by $\log K_{ow}$ (Booij et al., 2003). It has been shown above that for this
472 study, membrane resistance is negligible and calculation of the membrane resistance term is not
473 relevant. Further, we argue that $\log K_{ow}$ is generally not a good predictor neither for D_{LDPE} nor for
474 $K_{LDPE,w}$ values required for $R_{s,LDPE}$ calculation.

475 The model 'C' derives $k_{o,LDPE}$ under WBL control as a weak function of molar mass, but it suffers from
476 insufficient amount of available PRC data in the hydrophobicity range where partial dissipation (a
477 single compound), highly relevant for an improved model accuracy (Booij and Smedes, 2010), would
478 be expected.

479 Further, the accuracy of $k_{o,x}$ values largely depends on the quality of the $K_{x,w}$ values of the applied
480 PRCs (Equations 3 and 6). Booij and Smedes (2010) have shown that uncertainties in the $K_{x,w}$ values
481 of the PRCs may result in an $R_{s,x}$ bias of about 0.3 log units. Since $k_{o,SR}$ calculation (model 'A') is
482 derived from dissipation of more compounds than $k_{o,LDPE}$ (models 'B' and 'C'), the uncertainty of $k_{o,SR}$
483 is expected to be lower than that of $k_{o,LDPE}$. The accuracy of model fit largely depends on those PRCs

484 that dissipate from samplers between 20 and 80 %. In case of SR samplers, 2 to 5 PRCs fulfilled this
 485 criterion, whereas in LDPE samplers it was the case for only a single PRC. Furthermore, PCBs are
 486 generally considered to be more reliable PRCs than PAHs, mainly because of their better chemical
 487 stability. In view of the above mentioned uncertainties introduced by models 'B' and 'C', the model
 488 'A' seems to be the best option for derivation of $C_{w,LDPE}$.
 489 For PHE, sampling rate has no effect on the calculation of $C_{w,LDPE}$, since in all exposures, sampler has
 490 reached more than 90% partition equilibrium with water. This has been confirmed by an almost
 491 complete dissipation of d_{10} -PHE from LDPE in all exposures. For this compound, $C_{w,LDPE}$ can simply be
 492 calculated as $C_{w,LDPE} = C_{LPDE} / K_{LDPE,W}$. Thus, the accuracy of $C_{w,LDPE}$ estimate for PHE will strongly depend
 493 on the applied $K_{LDPE,W}$ value, whereas the accuracy of $C_{w,SR}$ depends mainly on the accuracy of the
 494 model that is used to derive the applied sampling rates (Lohmann et al., 2012). It has also been
 495 mentioned that the $C_{w,LDPE}$ and $C_{w,SR}$ values for PHE represent different periods of integrative
 496 sampling, and certain difference may reflect the temporal variability of PHE concentration in sampled
 497 water.



498
 Figure 7. Comparison of calculated free dissolved concentration in water $C_{w,x}$ (ng L^{-1}) of selected PAHs, and PCB 28 and HCB in LDPE and SR passive samplers deployed in DPS devices in 8 mobile and 2 stationary deployments. The dashed line represents equality of values. Sampling rates in LDPE were calculated using method 'A' outlined in 3.4.2.

499
 500 The results of this study as well as previous interlaboratory studies (Allan et al., 2009; Vrana et al.,
 501 2016), confirm a recommendation made by (Booij et al., 2017, 2016; Smedes et al., 2007) that
 502 standardization of $R_{s,x}$ estimation methods, improvement of analytical techniques, and the selection

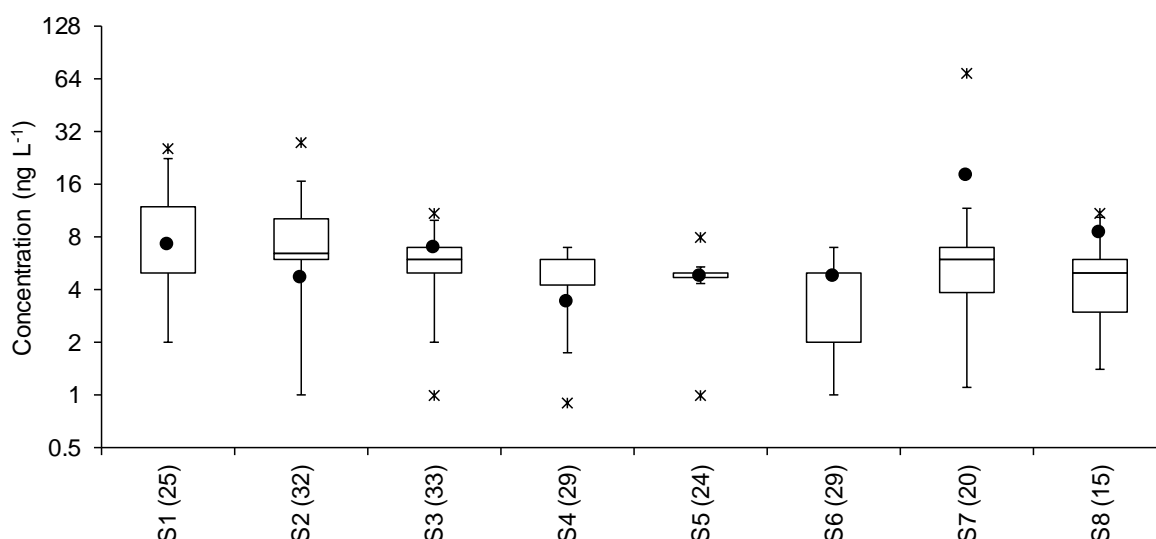
503 of high quality values for $K_{x,w}$ may greatly reduce interlaboratory variability of passive sampling
504 results.

505 4.3 Derivation of sampling rates for ED samplers

506
507 Since a good correlation was obtained for the $N_{t,x}/A_x$ ratio of co-deployed SR and ED samplers, in situ
508 cross-calibration was possible. The sampling rates of ED samplers $R_{s,ED}$ were estimated from sampling
509 rates derived for SR samplers ($R_{s,SR}$), using the calculated overall median $F_{ED/SR}$ ratio of 0.83, and the
510 surface areas of both samplers A_{ED} , A_{SR} :

$$R_{s,ED} = 0.83 \times \frac{A_{ED}}{A_{SR}} \times R_{s,SR} \quad \text{Equation 12}$$

511 The WBL controlled sampling rate estimate $R_{s,ED}$ obtained here should be from theory (Booij et al.,
512 2007) a function of the compound's diffusion coefficient in water and can be estimated for any
513 compound from its molar mass M using Equation 5.



514
515 Figure 8. Comparison of dissolved concentration of atrazine in water $C_{w,ED}$ ($\mu\text{g L}^{-1}$) estimated from ED
516 deployed in DPS devices in mobile exposures along 8 Danube stretches (S1-S8; black dots) with
517 concentrations in spot water samples collected during JDS3 survey within each stretch (box plots).
518 The box in the plot comprises data between 25th and 75th percentile (interquartile range; IQR) with
519 the median of the data shown by the horizontal line inside the box. The ends of whiskers represent
520 the range within 1.5 IQR of the lower and upper quartile, respectively. Extreme values found in spot
521 samples are labelled by asterisks. The numbers in brackets on x-axis denote the numbers of spot
522 samples analysed within each stretch.

523
524 The applicability of the outlined approach is demonstrated for the measurement of atrazine in 8
525 stretches of the Danube river (Figure 8). Atrazine was selected as a compound that was detectable in
526 all spot water samples and passive samplers. In each of the 8 stretches, the estimate of $C_{w,ED}$ for
527 atrazine lies within the range of concentration values measured in spot water samples collected
528 during JDS3 within the river stretches (ICPDR International Commission for the Protection of the
529 Danube River, n.d.).

530 When deriving free dissolved concentration from compound accumulation in ED, some limitations of
531 this approach have to be considered. These include uncertainty of the Empore disk uptake capacity,
532 since published values of Empore disk/water distribution coefficients are scarce and for polar
533 dissociating compounds they will be affected by compounds pK_a value and water pH. The assumption
534 of WBL controlled uptake may not be valid for all sampled compounds, especially those with low log
535 $K_{x,w}$ values. Despite these limitations we believe that free dissolved concentrations estimated using
536 the outlined cross-calibration approach provide values with lower uncertainty than those derived
537 from the currently most widely applied adsorption passive sampler, the POCIS (Miège et al., 2015).

538 **5 Conclusions and perspectives**

539 The main DPS usage domain is a representative measurement of compound levels, averaged in time
540 (TWA) and/or space. The DPS device presents a useful alternative approach to the conventional
541 sampler deployment technique in cages in situations where integrative uptake of compounds
542 accumulated under WBL control must be maximized.

543 We demonstrated the robustness of the DPS technique in stationary and mobile deployments in a
544 large river. When DPS is used for sampling from a cruising ship, the device may be, alternatively to
545 our deployment in a tank onboard a ship, directly immersed in the water column in front of the ship.
546 However, such deployment may be difficult in practice because the device may be easily damaged or
547 it may present an undesired obstacle to ship navigation.

548 Aqueous concentrations of PAHs, PCBs and HCB derived from DPS did not differ from those obtained
549 using conventional caged passive sampling. A good agreement was also found between aqueous
550 concentrations derived from DPS devices deployed from a cruising ship and those deployed from
551 river shore. The DPS sampled up to five times faster in comparison with a caged passive sampler
552 deployed in a streaming river water. This feature presents a great advantage for integrative sampling
553 of large equivalent volumes of water in a short time, when polymers with a high compound uptake
554 capacity ($K_{x,w} \times m_x$) are used. We expect even higher differences in sampling rates between DPS and
555 caged samplers when a comparison is performed under quiescent flow conditions.

556 The co-deployment of three passive samplers made of different sorbents in the DPS device, namely
557 SR, LDPE and ED, allowed to extend the range of sampled compounds from non-polar to more
558 hydrophilic ones. For all three co-deployed samplers we showed equivalent surface specific uptake
559 for compounds that were sampled integratively during the entire exposure period. This indicates that
560 mass transfer was dominantly WBL controlled and in such case the mass transfer coefficient is
561 equivalent for all applied sampler types. The differences in calculated aqueous concentrations
562 between LDPE and SR sampler were mainly associated with different applied uptake models. For
563 hydrophobic compounds, aqueous concentrations derived from SR and LDPE samplers uptake agreed
564 well when mass transfer coefficients derived for SR samplers were applied to the LDPE samplers.
565 The equivalent surface specific compound uptake provided a good basis for a cross-calibration
566 between the samplers and allowed derivation of aqueous concentrations also from compound
567 uptake in SDB-RPS Empore™ disks, for which the performance reference compound approach is not
568 applicable. We showed that aqueous atrazine concentrations derived from uptake by ED were in
569 good agreement with concentration obtained by spot sampling.

570 Besides mobile sampling in rivers or along lake or sea transects, application of the DPS can be
571 beneficial in scenarios with only short practicable deployment times or in lakes or water bodies with
572 low natural flow velocities, in cold/arctic conditions, everywhere where low sampling rates are

573 expected with caged passive samplers. The practical application of DPS is somewhat limited by the
574 need of external power source for driving the pump. Since strong water currents are created by
575 operation of the DPS device, it is not particularly suitable for investigation of depth chemical
576 stratification in stagnant water bodies. During deployment sampler exposure to sunlight is
577 minimised, and this effectively prevents photo degradation of compounds. The strong current inside
578 the exposure chamber minimises production of biofouling and samplers do not require extensive
579 cleaning even after long deployments.

580 **6 Acknowledgment**

581 We acknowledge the NORMAN association www.norman-network.net, the SOLUTIONS Project
582 supported by the European Union Seventh Framework Programme (FP7-ENV-2013-two-stage
583 Collaborative project) under grant agreement 603437. The research activities were carried out in the
584 RECETOX Research Infrastructure supported by the Czech Ministry of Education, Youth and Sports
585 (LM2015051) and the European Structural and Investment Funds, Operational Programme Research,
586 Development, Education (CZ.02.1.01/0.0/0.0/16_013/0001761). This work was also financially
587 supported by the Norwegian research council through NIVA's strategic priority research programme
588 (SIS Miljøgifter). We thank to Petra Příbylová, Petr Kukučka, Šimon Vojta, Ondřej Audy, Jiří Kohoutek,
589 Jitka Bečanová, Marek Pernica and Zdeněk Šimek from RECETOX, Masaryk University and Alfhild
590 Kringstad from NIVA for the instrumental analysis of samples and to Ondřej Sáňka from RECETOX,
591 Masaryk University for his assistance with preparation of Figure 2.

592 **Appendix A. Supplementary information**

593
594
595

596 7 References

- 597 Allan, I.J., Booij, K., Paschke, A., Vrana, B., Mills, G.A., Greenwood, R., 2009. Field performance of
598 seven passive sampling devices for monitoring of hydrophobic substances. *Environ. Sci.*
599 *Technol.* 43, 5383–5390.
- 600 Allan, I.J., Harman, C., 2011. Global aquatic passive sampling: maximizing available resources using a
601 novel exposure procedure. *Environ. Sci. Technol.* 45, 6233–4.
602 <https://doi.org/10.1021/es2021022>
- 603 Allan, I.J., Harman, C., Ranneklev, S.B., Thomas, K. V, Grung, M., 2013. Passive sampling for target and
604 nontarget analyses of moderately polar and nonpolar substances in water. *Environ. Toxicol.*
605 *Chem.* 32, 1718–26. <https://doi.org/10.1002/etc.2260>
- 606 Allan, I.J., Nilsson, H.C., Tjensvoll, I., Bradshaw, C., Næs, K., 2011. Mobile passive samplers: Concept
607 for a novel mode of exposure. *Environ. Pollut.* 159, 2393–2397.
608 <https://doi.org/10.1016/j.envpol.2011.06.039>
- 609 Booij, K., Hofmans, H.E., Fischer, C. V, van Weerlee, E.M., 2003. Temperature-Dependent Uptake
610 Rates of Nonpolar Organic Compounds by Semipermeable Membrane Devices and Low-Density
611 Polyethylene Membranes. *Environ. Sci. Technol.* 37, 361–366.
- 612 Booij, K., Robinson, C.D., Burgess, R.M., Mayer, P., Roberts, C.A., Ahrens, L., Allan, I.J., Brant, J., Jones,
613 L., Kraus, U.R., Larsen, M.M., Lepom, P., Petersen, J., Pröfrock, D., Roose, P., Schäfer, S.,
614 Smedes, F., Tixier, C., Vorkamp, K., Whitehouse, P., 2016. Passive Sampling in Regulatory
615 Chemical Monitoring of Nonpolar Organic Compounds in the Aquatic Environment. *Environ. Sci.*
616 *Technol.* 50, 3–17. <https://doi.org/10.1021/acs.est.5b04050>
- 617 Booij, K., Smedes, F., 2010. An improved method for estimating in situ sampling rates of nonpolar
618 passive samplers. *Environ. Sci. Technol.* 44, 6789–6794.
- 619 Booij, K., Smedes, F., Crum, S., 2017. Laboratory performance study for passive sampling of nonpolar
620 chemicals in water. *Environ. Toxicol. Chem.* 36, 1156–1161. <https://doi.org/10.1002/etc.3657>
- 621 Booij, K., Vrana, B., Huckins, J.N., 2007. Theory, modelling and calibration of passive samplers used in
622 water monitoring, in: Greenwood, R., Mills, G., Vrana, B. (Eds.), *Comprehensive Analytical*
623 *Chemistry* 48. *Passive Sampling Techniques in Environmental Monitoring*. Elsevier, Amsterdam,
624 pp. 141–169. [https://doi.org/10.1016/S0166-526X\(06\)48007-7](https://doi.org/10.1016/S0166-526X(06)48007-7)
- 625 Deutsch, K., Sengl, M., 2015. Priority and other organic substances, in: Liška, I., Wagner, F., Sengl, M.,
626 Deutsch, K., Slobodník, J. (Eds.), *Joint Danube Survey 3. A Comprehensive Analysis of Danube*
627 *Water Quality*. ICPDR – International Commission for the Protection of the Danube River,
628 Vienna, pp. 211–222.
- 629 Estoppey, N., Schopfer, A., Omlin, J., Esseiva, P., Vermeirssen, E.L.M., Delémont, O., de Alencastro,
630 L.F., 2014. Effect of water velocity on the uptake of polychlorinated biphenyls (PCBs) by silicone
631 rubber (SR) and low-density polyethylene (LDPE) passive samplers: An assessment of the
632 efficiency of performance reference compounds (PRCs) in river-like flow condition. *Sci. Total*
633 *Environ.* 499, 319–326. <https://doi.org/10.1016/j.scitotenv.2014.08.047>
- 634 EU, 2013. Directive 2013/39/EU of the European Parliament and of the Council of 12 August 2013
635 amending Directives 2000/60/EC and 2008/105/EC as regards priority substances in the field of
636 water policy. *Off. J. Eur. Union* L226, 1–17.
- 637 EU, 2000. Directive 2000/60/EC of the European parliament and of the council of 23 October 2000
638 establishing a framework for community action in the field of water policy. *Off. J. Eur. Union*
639 L327, 1–72.
- 640 ICPDR International Commission for the Protection of the Danube River, n.d. Danube River Basin
641 Water Quality Database [WWW Document]. URL <http://www.icpdr.org/wq-db/> (accessed
642 2.3.18).
- 643 Jahnke, A., MacLeod, M., Wickström, H., Mayer, P., 2014. Equilibrium Sampling to Determine the
644 Thermodynamic Potential for Bioaccumulation of Persistent Organic Pollutants from Sediment.
645 *Environ. Sci. Technol.* 48, 11352–11359. <https://doi.org/10.1021/es503336w>
- 646 Levich, V.G., 1962. Convective diffusion in liquids, in: *Physicochemical Hydrodynamics*. Prentice-Hall,

647 Englewood Cliffs, N.J., pp. 139–183.

648 Li, H., Vermeirssen, E.L., Helm, P.A., Metcalfe, C.D., 2010. Controlled field evaluation of water flow
649 rate effects on sampling polar organic compounds using polar organic chemical integrative
650 samplers. *Environ. Toxicol. Chem.* 29, 2461–2469.

651 Liška, I., Wagner, F., Sengl, M., Deutsch, K., Slobodník, J., 2015. Joint Danube Survey 3. A
652 comprehensive analysis of Danube water quality. ICPDR – International Commission for the
653 Protection of the Danube River, Vienna.

654 Lohmann, R., Booij, K., Smedes, F., Vrana, B., 2012. Use of passive sampling devices for monitoring
655 and compliance checking of POP concentrations in water. *Environ. Sci. Pollut. Res. Int.* 19,
656 1885–95. <https://doi.org/10.1007/s11356-012-0748-9>

657 Miège, C., Mazzella, N., Allan, I., Dulio, V., Smedes, F., Tixier, C., Vermeirssen, E., Brant, J., O’Toole, S.,
658 Budzinski, H., Ghestem, J.-P., Staub, P.-F., Lardy-Fontan, S., Gonzalez, J.-L., Coquery, M., Vrana,
659 B., 2015. Position paper on passive sampling techniques for the monitoring of contaminants in
660 the aquatic environment - Achievements to date and perspectives. *Trends Environ. Anal. Chem.*
661 8, 20–26. <https://doi.org/10.1016/j.teac.2015.07.001>

662 Petersen, J., Pröfrock, D., Paschke, A., Broekaert, J.A.C., Prange, A., 2016. Development and field test
663 of a mobile continuous flow system utilizing Chemcatcher for monitoring of rare earth elements
664 in marine environments. *Environ. Sci. Water Res. Technol.* 2, 146–153.
665 <https://doi.org/10.1039/C5EW00126A>

666 Petersen, W., 2014. FerryBox systems: State-of-the-art in Europe and future development. *J. Mar.*
667 *Syst.* 140, 4–12. <https://doi.org/10.1016/j.jmarsys.2014.07.003>

668 Qin, Z., Bragg, L., Ouyang, G., Niri, V.H., Pawliszyn, J., 2009. Solid-phase microextraction under
669 controlled agitation conditions for rapid on-site sampling of organic pollutants in water. *J.*
670 *Chromatogr. A* 1216, 6979–6985. <https://doi.org/10.1016/j.chroma.2009.08.052>

671 Reichenberg, F., Mayer, P., 2006. Two complementary sides of bioavailability: accessibility and
672 chemical activity of organic contaminants in sediments and soils. *Environ. Toxicol. Chem.* 25,
673 1239–45.

674 Rusina, T., Smedes, F., Klanova, J., 2010. Diffusion coefficients of polychlorinated biphenyls and
675 polycyclic aromatic hydrocarbons in polydimethylsiloxane and low-density polyethylene
676 polymers. *J. Appl. Polym. Sci.* 116, 1803–1810.

677 Rusina, T., Smedes, F., Klanova, J., Booij, K., Holoubek, I., 2007. Polymer Selection for Passive
678 Sampling: a Comparison of Critical Properties. *Chemosphere* 68, 1344–1351.

679 Rusina, T., Smedes, F., Koblizkova, M., Klanova, J., 2010. Calibration of silicone rubber passive
680 samplers: Experimental and modeled relations between sampling rate and compound
681 properties. *Environ. Sci. Technol.* 44, 362–367.

682 Salaun, P., Buffle, J., 2004. Integrated Microanalytical System Coupling Permeation Liquid Membrane
683 and Voltammetry for Trace Metal Speciation. Theory and Applications. *Anal. Chem.* 76, 31–39.

684 Shaw, M., Eaglesham, G., Mueller, J.F., 2009. Uptake and release of polar compounds in SDB-RPS
685 Empore™ disks; implications for their use as passive samplers. *Chemosphere* 75, 1–7.
686 <https://doi.org/10.1016/j.chemosphere.2008.11.072>

687 Smedes, F., Booij, K., 2012. Guidelines for passive sampling of hydrophobic contaminants in water
688 using silicone rubber samplers [WWW Document]. URL
689 <http://www.rs.passivesampling.net/PSguidanceTimes52.pdf>

690 Smedes, F., Geertsma, R.W., Van Der Zande, T., Booij, K., 2009. Polymer-water partition coefficients
691 of hydrophobic compounds for passive sampling: Application of cosolvent models for
692 validation. *Environ. Sci. Technol.* 43, 7047–7054.

693 Smedes, F., Zande, T. van der, Roose, P., Davies, I.M., 2007. ICES Passive sampling trial survey for
694 water and sediment (PSTS) 2006 – 2007. Part 3: Preliminary interpretation of field data [WWW
695 Document]. URL <http://www.ices.dk/sites/pub/CM Documents/CM-2007/J/J0407.pdf>
696 (accessed 2.2.18).

697 Ter Laak, T.L., Busser, F.J.M., Hermens, J.L.M., 2008. Poly(Dimethylsiloxane) as Passive Sampler
698 Material for Hydrophobic Chemicals: Effect of Chemical Properties and Sampler Characteristics

699 on Partitioning and Equilibration Times. *Anal. Chem.* 80, 3859–3866.

700 Umlauf, G., Giulio, M., Helle, S., 2015. Spatial and temporal trends of Dioxins, PCBs and BDE-209 in
701 suspended particulate matter and fish – JDS3 versus JDS2, in: Liška, I., Wagner, F., Sengl, M.,
702 Deutsch, K., Slobodník, J. (Eds.), *Joint Danube Survey 3. A Comprehensive Analysis of Danube*
703 *Water Quality*. ICPDR – International Commission for the Protection of the Danube River,
704 Vienna, pp. 249–259.

705 Vermeirssen, E.L.M., Bramaz, N., Hollender, J., Singer, H., Escher, B.I., 2009. Passive sampling
706 combined with ecotoxicological and chemical analysis of pharmaceuticals and biocides -
707 evaluation of three Chemcatcher configurations. *Water Res.* 43, 903–14.
708 <https://doi.org/10.1016/j.watres.2008.11.026>

709 Vrana, B., Allan, I.J., Greenwood, R., Mills, G.A., Dominiak, E., Svensson, K., Knutsson, J., Morrison, G.,
710 2005. Passive sampling techniques for monitoring pollutants in water. *TrAC - Trends Anal.*
711 *Chem.* 24, 845–868.

712 Vrana, B., Klučárová, V., Benická, E., Abou-Mrad, N., Amdany, R., Horáková, S., Draxler, A., Humer, F.,
713 Gans, O., 2014. Passive sampling: An effective method for monitoring seasonal and spatial
714 variability of dissolved hydrophobic organic contaminants and metals in the Danube river.
715 *Environ. Pollut.* 184, 101–112.

716 Vrana, B., Schüürmann, G., 2002. Calibrating the uptake kinetics of semipermeable membrane
717 devices in water: Impact of hydrodynamics. *Environ. Sci. Technol.* 36, 290–296.

718 Vrana, B., Smedes, F., Prokeš, R., Loos, R., Mazzella, N., Mieke, C., Budzinski, H., Vermeirssen, E.,
719 Ocelka, T., Gravell, A., Kaserzon, S., 2016. An interlaboratory study on passive sampling of
720 emerging water pollutants. *TrAC Trends Anal. Chem.* 76, 153–165.
721 <https://doi.org/10.1016/j.trac.2015.10.013>
722

Supplementary material for on-line publication only

[Click here to download Supplementary material for on-line publication only: Supplementary_information_revised_r2.DOCX](#)

Meta data for sampling stretches, as described in Table 1

[Click here to download Interactive Map file \(.kml or .kmz\): DANUBE2013.kmz](#)